Check for updates

Angewandte Chemie International Edition

Angewandte International Edition Chemie

GDCh German Chemical Society

How to cite: *Angew. Chem. Int. Ed.* **2026**, e1500194
doi.org/10.1002/anie.1500194

RESEARCH ARTICLE

Automated Solid-Phase Flow Synthesis for Scaffold Diversification of a High-Throughput Screening Hit

Zhenyang Yu[1,2] | Zhi-Qi Zhang[1] | Jiale Wu[1] | Yanbin Zhang[1] | Hwee Ting Ang[1] | Feng Zhou[1] | Jackie Ang[3] | Mei Yee Wong[3] | Ronald Toh Kuan Hai[3] | Frankie S Mak[3] | Jie Wu[1,2]

[1]Department of Chemistry, National University of Singapore, Singapore, Singapore | [2]National University of Singapore (Chongqing) Research Institute, Chongqing, China | [3]Experimental Drug Development Centre (EDDC), Agency for Science, Technology and Research (A*STAR), Chromos, Singapore

Correspondence: Frankie S Mak (frankie_mak@eddc.sg) | Jie Wu (chmjie@nus.edu.sg)

Received: 24 July 2026 | **Revised:** 19 October 2026 | **Accepted:** 21 October 2026

Keywords: automated synthesis | chemical recipe file | flow chemistry | medicinal chemistry | solid-phase synthesis

ABSTRACT

High-throughput screening (HTS) enables rapid hit identification, yet subsequent analogue synthesis and structure–activity relationship exploration remain constrained by labor-intensive multistep workflows. Here, we describe an automated solid-phase flow synthesis (SPS-flow) platform for diversity-oriented analogue generation of an HTS-derived, non-peptidic small-molecule hit scaffold. A benzodiazepine hit against cyclin-dependent kinase 11B (CDK11B) was selected as a proof-of-concept and translated into a modular 10–11-step synthetic sequence through fragment-guided retrosynthetic design. A sterically tuned triazene linker on 2-chlorotrityl resin was developed to tolerate diverse reaction conditions while enabling traceless cleavage and post-synthetic diazonium diversification, and Chemical Recipe File (CRF)-based control coordinated continuous-, circulation-, and stop-flow operations within a unified automated workflow. The platform enabled the synthesis of 42 benzodiazepine analogues in 5%–33% overall yields, with each sequence completed within approximately 45–48 h from a common resin-bound precursor. Within the explored first-generation design space, the library rapidly defined the synthetic accessibility and preliminary structure–activity landscape of the scaffold under SPS-flow conditions, supporting early triage of the series and demonstrating that SPS-flow can be used as a programmable platform for automated multistep diversification and early-stage drug optimization.

1 | Introduction

High-throughput screening (HTS) has transformed early drug discovery by enabling rapid identification of hit compounds against diverse biological targets. However, converting these hits into informative structure–activity relationships (SAR) still largely depends on manual, multistep synthesis and purification, which are slow, labor-intensive, and difficult to standardize or automate [1–3]. This bottleneck is particularly acute for diversification of HTS-derived scaffolds, where efficient exploration of scaffold-level chemical space around promising hits is essential for assessing scaffold tractability and making informed go/no-go decisions [4].

A variety of automated synthesis platforms have been developed for single-target route optimization and for the production of small sets of derivatives, but most are designed around specific targets and routes rather than around HTS hit scaffolds. Automated batch and flow systems have already enabled robust single-step optimization and route-specific multistep synthesis for selected targets [5–11]. Yet most implementations rely on complex, fixed architectures with inline analytics, scavenger

Zhenyang Yu and Zhi-Qi Zhang contributed equally to this study.

All rights reserved, including rights for text and data mining and training of artificial intelligence technologies or similar technologies.
© 2026 Wiley-VCH GmbH

columns, or regeneration modules tailored to a specific route [12], which can limit their adaptability for scaffold-level diversification. The radial synthesizer developed by Gilmore and co-workers further demonstrated automated linear and convergent multistep synthesis and analogue generation through a reconfigurable flow architecture [13]. While such advances have improved the flexibility of automated multistep synthesis, intermediate handling and purification remain important considerations in the development of integrated synthetic workflows.

Solid-phase flow synthesis (SPS-flow) for complex small molecules was developed by our group to address this need by combining the purification efficiency of solid-phase synthesis (SPS) with the control and automation of flow chemistry. In SPS, resin-bound intermediates can be purified by simple filtration and washing, minimizing chromatographic operations [14–16], while flow operation affords precise control over reaction parameters, efficient heat and mass transfer, and straightforward integration with digital control [17, 18]. Merging these concepts, SPS-flow executes multistep synthetic sequences on resin under recirculating-flow conditions, governed by digitally encoded programs, and thereby provides a programmable framework for chromatography-free multistep automation, particularly for synthesis of polypeptide and oligonucleotide [19–21].

Our previous work has shown that SPS-flow can deliver complex small molecules under the control of a Chemical Recipe File (CRF) (Figure 1). In the first study, a fully automated six-step synthesis of prexasertib and selected derivatives demonstrated that continuous-flow solid-phase synthesis can access a clinically relevant drug candidate from a common resin-bound intermediate, using a single CRF to control all reagent additions, washes, and temperature profiles [22]. Early- and late-stage diversification were implemented by swapping building blocks at defined positions in the CRF, allowing analogue generation without redesigning the underlying multistep sequence. In the second study, SPS-flow was applied to antiviral peptidomimetics using a compact parallel synthesizer. Iterative amide-coupling and deprotecting steps encoded in CRFs enabled "button-push" construction of α-keto-amide and nitrile peptidomimetics libraries guided by docking simulations, with five distinct molecules produced per cycle and 42 derivatives prepared over 3 months for SAR optimization [23]. Together, these studies established SPS-flow as an automated platform for analogue synthesis across predefined small-molecule and peptide-like scaffolds. Nevertheless, its application to scaffold-level appendage or functional-group diversification centered on HTS-derived hit scaffolds in early-stage drug discovery remained unexplored.

Here, SPS-flow is extended from target- and route-focused multistep synthesis to scaffold-level diversity-oriented analogue generation from HTS-derived hit scaffolds in an early-stage drug discovery context (Figure 1). As a demanding proof-of-concept, a tetrahydro-1,4-benzodiazepine (hereafter referred to as benzodiazepine) core identified as a cyclin dependent kinase 11B (CDK11B) hit from an in-house HTS campaign was selected, providing a realistic scaffold for testing whether SPS-flow can support scaffold diversification and triage at the hit stage. A fragment-guided retrosynthetic design was formulated to expose multiple diversification sites along a 10–11-step sequence. To realize this multistep scaffold diversification workflow, a sterically tuned triazene linker on 2-chlorotrityl resin was engineered to withstand strong electrophiles and Lewis-acidic borane conditions while permitting traceless cleavage into diazonium intermediates, and CRF-encoded operation was implemented across continuous-, circulation-, and stop-flow modes selected according to the requirements of each transformation. Applied to the CDK11B benzodiazepine scaffold, the resulting SPS-flow platform constructs a 42-member analogue library within approximately 45–48 h per sequence, with a single final purification step and modest solvent consumption, furnishing an initial analogue set for scaffold triage and for probing initial SAR trends across the accessible diversification sites.

2 | Results and Discussion

To demonstrate the capability of SPS-flow to support automated analogue diversification around realistic medicinal chemistry scaffolds, an HTS-derived benzodiazepine hit against cyclin dependent kinase 11B (CDK11B) was chosen as a proof-of-concept substrate. Cyclin-dependent kinases (CDKs) are serine/threonine kinases that operate as cyclin-associated heterodimers and play central roles in cell-cycle control and transcriptional regulation [24]. Dysregulation of CDK activity undermines checkpoint control and drives uncontrolled proliferation, and aberrant CDK expression is therefore a common feature of many cancers [25]. Within this family, CDK11 has only recently come into focus as an oncology target [26]. Functional studies have shown that CDK11B supports tumor cell survival and growth in several indications, and that genetic or pharmacological suppression reduces viability in preclinical models [27, 28]. Current reviews and translational projects describe CDK11 as a novel anti-cancer strategy and highlight that work is still centered on understanding its biology and discovering selective inhibitors, with no CDK11-targeted drugs yet approved [29, 30]. The CDK11B program is therefore firmly positioned at an early stage of drug discovery, where rapid assessment of scaffold tractability and exploratory SAR are particularly valuable.

Given this emerging target profile, an in-house HTS campaign was undertaken to identify CDK11B hit scaffolds suitable for SPS-flow-enabled diversification. A Nano-BRET Intracellular Kinase Assay optimized (Figure S1) for CDK11B was used to screen 100,160 compounds, yielding 406 primary hits with more than 50% inhibition at 10 μM. Retesting and dose–response profiling reduced this to 96 verified hits, which were grouped into structurally distinct clusters by chemoinformatic analysis. From these clusters, a benzodiazepine chemotype represented by compound **1** was selected because it combined measurable CDK11B inhibition (IC_{50} = 1.8 μM), clear structural differentiation from reported CDK inhibitor chemotypes [31], and multiple positions that could be diversified within a modular synthetic design (Figure 2). In addition, this chemotype is complementary to our virtual-screening-derived hit-finding approach for CDK11B, further supporting its selection as a representative scaffold for methodological evaluation [32].

Retrosynthetic analysis revealed that the target scaffold can be modularly assembled from three key fragments: a benzodiazepine core, five-membered heteroaromatic unit, and an amine substituent. The benzodiazepine core is accessible from anthranilic

15213773, 0, Downloaded from https://onlinelibrary.wiley.com/doi/10.1002/anie.1500194 by National University Of Singapore, Wiley Online Library on [29/10/2026]. See the Terms and Conditions (https://onlinelibrary.wiley.com/terms-and-conditions) on Wiley Online Library for rules of use; OA articles are governed by the applicable Creative Commons License

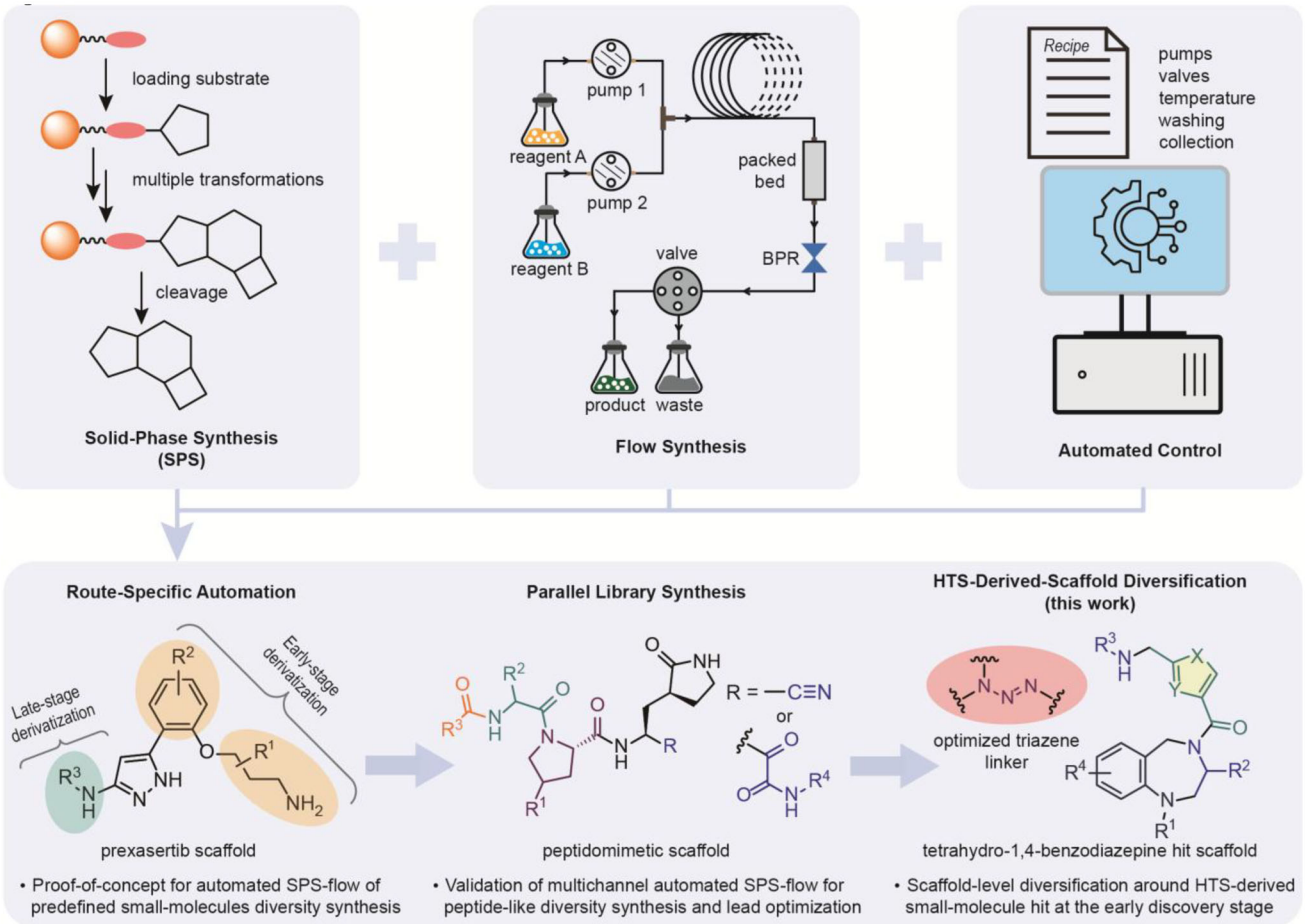


FIGURE 1 | Evolution of the SPS-flow platform in scope and application. Integration of solid-phase synthesis, flow chemistry, and automated control enables programmable multistep synthesis. Previous applications in route-specific automation and parallel library synthesis are extended in this work to automated diversification of a high-throughput screening (HTS)-derived hit scaffold.

acid, aliphatic aldehydes, and α-amino acids (Figure S2a). This disconnection pattern was particularly attractive for diversity-oriented analogue synthesis because it distributed diversification opportunities across both early and late stages of the sequence, allowing analogue generation through systematic variation of aldehydes, amino acids, heteroaromatic components, amines, and post-cleavage diazonium transformations. The scaffold therefore provided a practical entry point for SPS-flow-enabled analogue generation from a medicinally relevant HTS hit.

A central challenge in translating this design into SPS-flow was a linker and resin system that could survive chemically distinct transformations while preserving the diversification logic of the scaffold. To this end, a sterically tuned triazene linker was constructed by functionalizing 2-chlorotrityl chloride resin **2** with a triacetonediamine **3** and aryldiazonium salt **5** (Figure 3a). The modified resin **6** achieved substrate loadings of up to 0.8 mmol/g, as determined by cleavage of the 2-nitrobenzoic acid aryldiazonium from the resin using 5% TFA/DCM followed by reduction (Figure S7). The steric environment and electronic properties of this triazene linker were selected to improve stability under strongly electrophilic and Lewis-acidic conditions (Figure S4), while still permitting traceless cleavage into aryldiazonium intermediates for post-synthetic diversification [33]. The choice of 2-chlorotrityl resin was guided by resin swelling, chemical compatibility, and loading performance, which together provided a robust physical platform for multistep SPS-flow synthesis (Figure S3 and Table S1) [34, 35].

With this resin–linker system in place, the multistep sequence was encoded into a unified digital workflow as a CRF, specifying reagent delivery, washing operations, temperature, and the appropriate flow mode for each step. The automated operation of the SPS-flow platform is demonstrated in the Supplementary Movie. Continuous-flow operation was used for fast transformations such as nitro reduction, circulation-flow was used for longer residence steps such as reductive amination and coupling and stop-flow was required for the heated $Me_2S{\bullet}BH_3$-mediated lactam reduction that formed the benzodiazepine core.

The synthesis route to compound **1** was first validated in batch solution-phase (Figure S2b) and then translated into SPS-flow format. Most transformations could be carried over directly, but several operations required adjustment for SPS-flow compatibility, including premixed delivery of the nitro-reduction reagents, washing after imine formation prior to $NaBH_3CN$ addition, and staged handling of $Me_2S{\bullet}BH_3$ to manage gas evolution before heating under stop-flow conditions. With further optimization of the SPS-flow conditions (Tables S2–S9), compound **1** was obtained in 32% overall yield after a single final purification by

15213773, 0, Downloaded from https://onlinelibrary.wiley.com/doi/10.1002/anie.1500194 by National University Of Singapore, Wiley Online Library on [29/10/2026]. See the Terms and Conditions (https://onlinelibrary.wiley.com/terms-and-conditions) on Wiley Online Library for rules of use; OA articles are governed by the applicable Creative Commons License

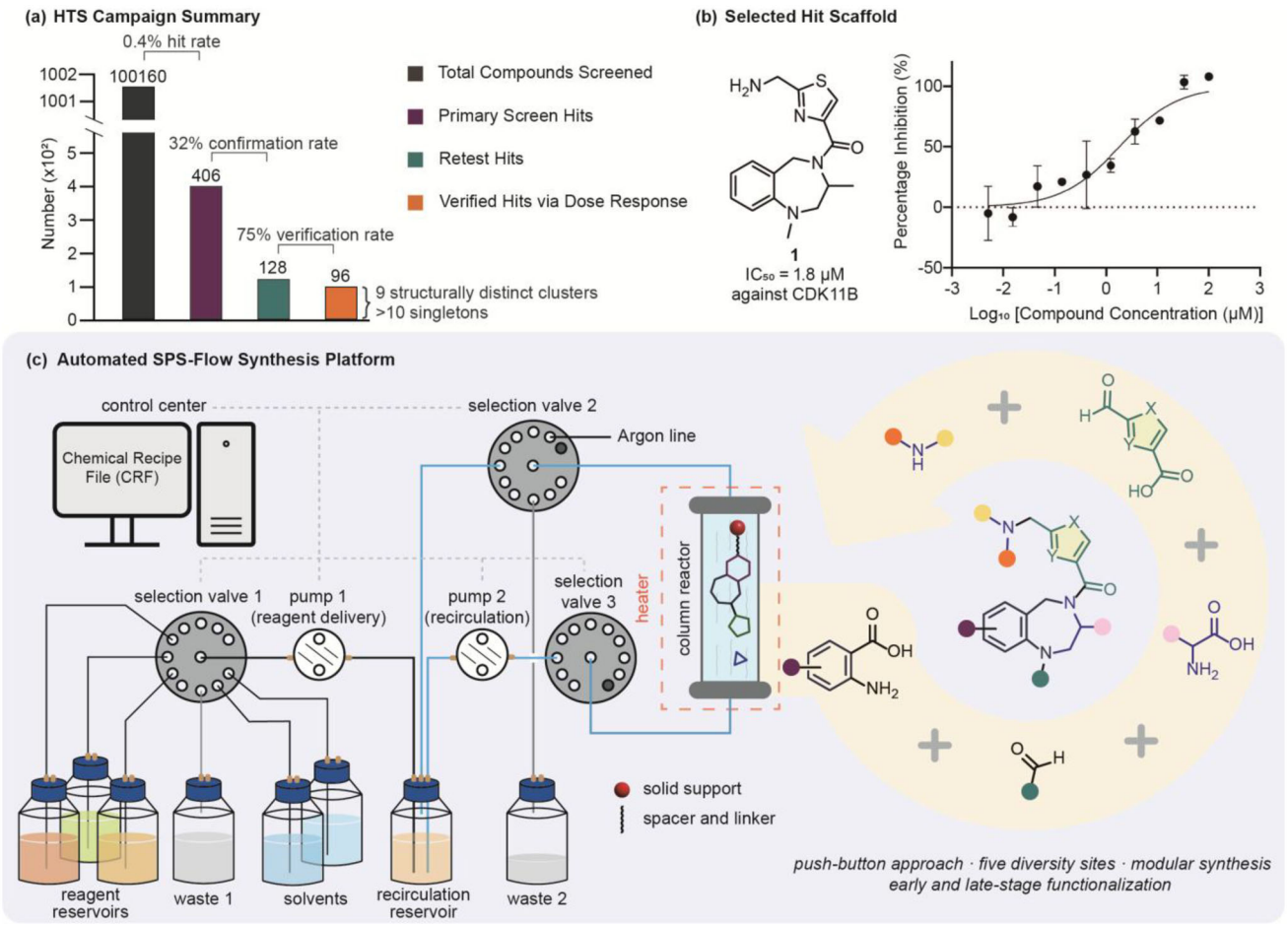


FIGURE 2 | HTS-derived CDK11B benzodiazepine hit and automated SPS-flow platform. (a) Summary of the in-house HTS campaign for CDK11B. (b) Structure and dose–response profile of the selected benzodiazepine hit for SPS-flow diversification. (c) Schematic of the automated SPS-flow platform and five diversification sites for early- and late-stage functionalization.

preparative HPLC after cleavage (Figure S12), compared with 28% overall yield for the corresponding batch route. The SPS-flow sequence not only minimized the purification burden by keeping intermediates resin-bound throughout the multistep process but also required only modest solvent consumption (Table S11). These results show that the synthesis route is compatible with automated SPS-flow operation while maintaining or slightly improving overall efficiency relative to batch.

Building on the optimized SPS-flow route to compound **1**, the resulting CRF encoded a nine-step core synthetic sequence (Figure 3b) that served as the programmable backbone for scaffold-level diversification around the benzodiazepine hit. Resin-bound nitrobenzene **6** was reduced to the corresponding aniline **7** using $B_2(OH)_4$, catalyzed by 4,4'-bipyridine, under continuous-flow mode, as the highly reactive species generated in situ enabled complete conversion within minutes [36]. Compound **7** underwent reductive amination to give amine **8**. Subsequent acylation with Fmoc-amino acid chloride **9** and deprotection afforded **11**, which cyclized intramolecularly to lactam **12**. These steps were performed under circulation-flow mode to ensure sufficient reaction time for complete conversion.

Lactam **12** was next transformed into diamine **13** by $Me_2S{\bullet}BH_3$-mediated reduction of both lactam moieties. Batch studies showed that complete reduction of the two lactam moieties requires heating at 70°C in a sealed flask (Figure S2b). In the SPS-flow system, this transformation was therefore implemented under stop-flow mode, allowing efficient reduction of the solid-supported lactams to form the benzodiazepine core while maintaining a high concentration of $Me_2S{\bullet}BH_3$ at 70°C [37]. To maintain compatibility with the triazene linker, the amine–borane complexes formed during the reduction—typically hydrolyzed with hydrochloric acid under reflux—were instead treated with a 50% THF solution of *N,N,N',N'*-tetramethyl ethylenediamine (TMEDA), smoothly releasing the corresponding amines **13** under linker-compatible conditions [38]. Under circulation-flow conditions, coupling with heteroaromatic fragment **14** followed by reductive amination furnished **16**, which, upon cleavage with 5% TFA in DCM, produced aryldiazonium intermediate **17**. This intermediate could undergo diverse transformations, including reduction [39] and Sandmeyer reactions [40], to deliver targeted benzodiazepine derivatives **18**.

Using the benzodiazepine CRF as a common backbone, the SPS-flow platform was then applied to analogue generation across five diversification points. Variations in aldehyde (**D1–D5**), amino acid (**D6–D12**), heteroaromatic unit (**D13–D15**), and amine building blocks (**D16–D33**), together with an additional amide-coupling branch (Figure S14, **D34–D40**) and post cleavage

15213773, 0, Downloaded from https://onlinelibrary.wiley.com/doi/10.1002/anie.1500194 by National University Of Singapore, Wiley Online Library on [29/10/2026]. See the Terms and Conditions (https://onlinelibrary.wiley.com/terms-and-conditions) on Wiley Online Library for rules of use; OA articles are governed by the applicable Creative Commons License

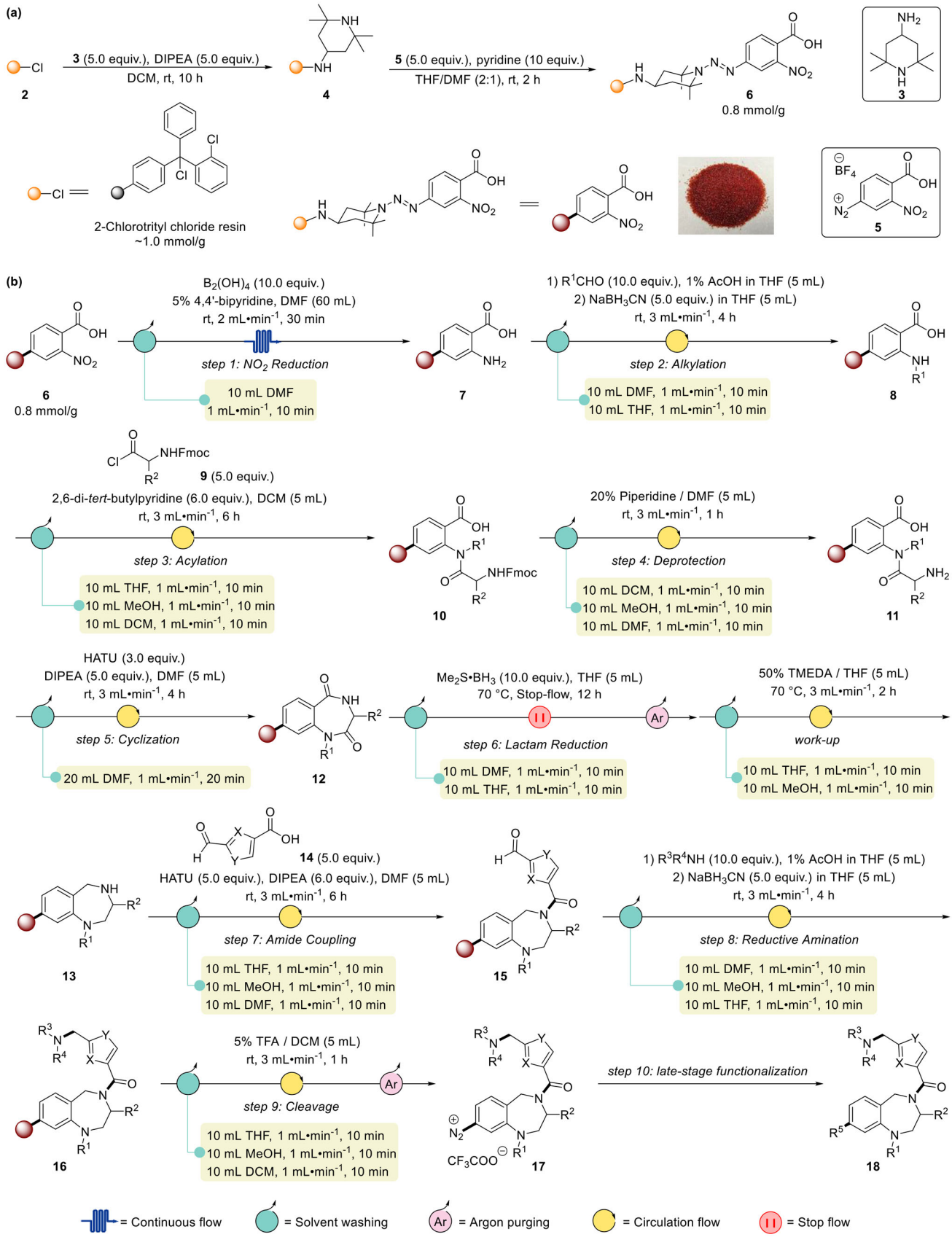


FIGURE 3 | Triazene linker design and unified CRF for benzodiazepine synthesis. (a) Preparation of the sterically bulky triazene linker and modified resins. (b) Chemical Recipe File (CRF)-encoded synthetic sequence illustrating the integration of continuous-flow, circulation-flow, and stop-flow operations, together with intermediate washing and argon purging, within a unified automated workflow. The symbols and color coding indicate the corresponding operating modes and processing steps.

15213773, 0, Downloaded from https://onlinelibrary.wiley.com/doi/10.1002/anie.15001194 by National University Of Singapore, Wiley Online Library on [29/10/2026]. See the Terms and Conditions (https://onlinelibrary.wiley.com/terms-and-conditions) on Wiley Online Library for rules of use; OA articles are governed by the applicable Creative Commons License

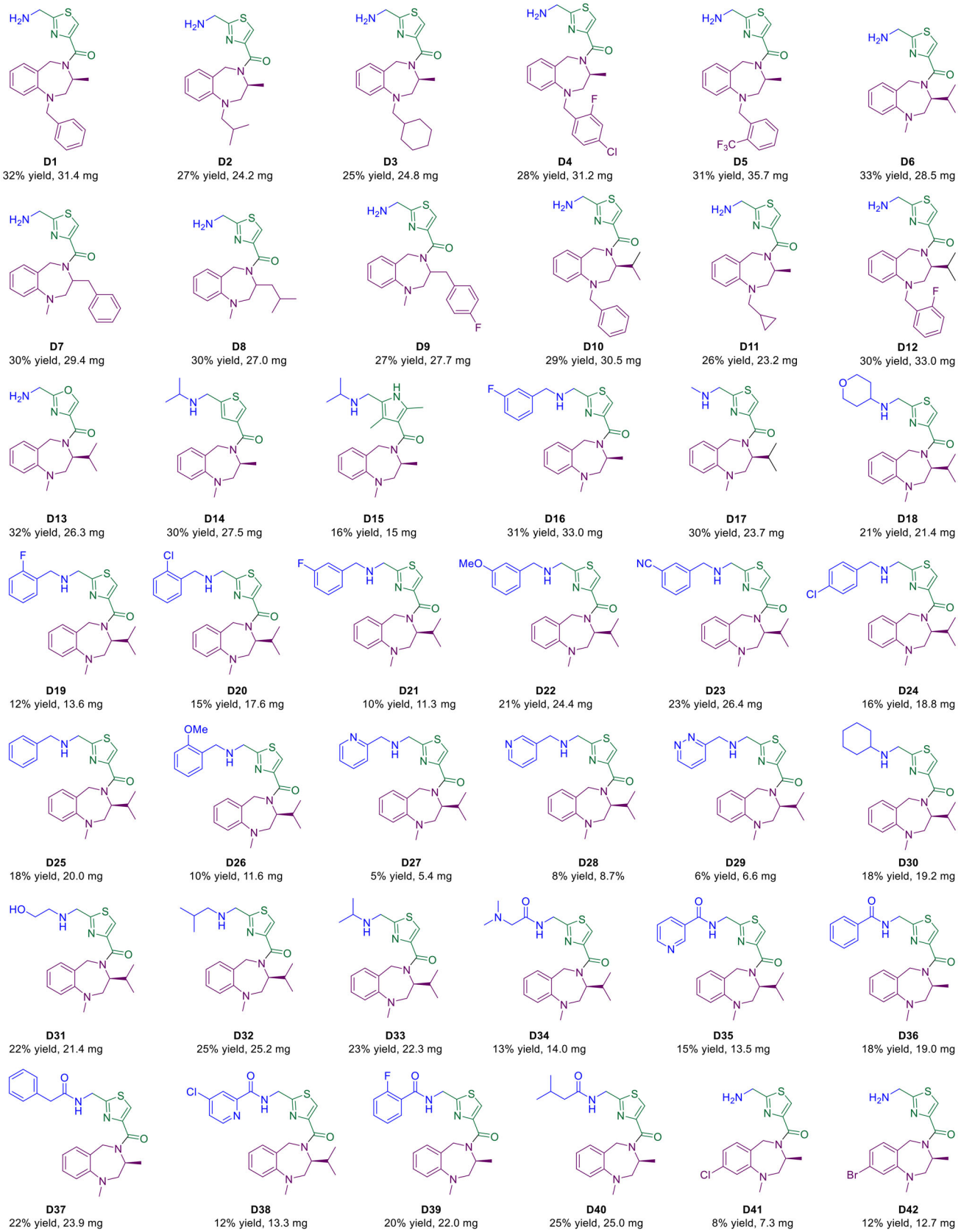


FIGURE 4 | Automated SPS-flow synthesis of benzodiazepine derivatives with the established CRF. Overall isolated yields and corresponding product masses are provided for each derivative. All syntheses were performed from a common resin-bound precursor, with each sequence involving 10–11 synthetic steps and a single final purification.

15213773, 0, Downloaded from https://onlinelibrary.wiley.com/doi/10.1002/anie.15001194 by National University Of Singapore, Wiley Online Library on [29/10/2026]. See the Terms and Conditions (https://onlinelibrary.wiley.com/terms-and-conditions) on Wiley Online Library for rules of use; OA articles are governed by the applicable Creative Commons License

diazonium transformations (**D41** and **D42**), enabled the synthesis of 42 benzodiazepine derivatives through 10–11-step sequences (Figure 4). Each sequence was completed within approximately 45–48 h. All compounds were prepared from 300 mg of resin **6**, and yields were calculated based on a starting material loading of 0.8 mmol/g. The final compounds were obtained in 5%–33% overall yield after a single purification step.

The library synthesis also showed which parts of the scaffold are currently accessible under the platform. Bulky five-membered heterocycles showed reduced compatibility in the amide-coupling step, likely reflecting steric limitations during fragment installation, whereas aromatic heterocyclic benzylamines were less successful in the reductive amination step, consistent with less favorable imine formation or stability. The failed examples (Figure S15) also indicated that alkylation in step 2 was indispensable for the synthetic route, whereas aniline was incompatible with the transformation in step 8. As a result, the campaign helps clarify where the present SPS-flow sequence operates reliably and where additional methodological development would be required to access new analogue space, providing a practical view of scaffold positions and reagent classes that are currently compatible with the SPS-flow sequence. Taken together, these results demonstrate diversity-oriented analogue generation around a representative benzodiazepine scaffold by swapping building blocks within a fixed digital workflow, enabling exploration of multiple diversification vectors through a complex multistep sequence. Although ultra-performance liquid chromatography–mass spectrometry (UPLC-MS) analyses and characterization of selected intermediates support reaction progression, comprehensive assessment of incomplete conversions and resin-bound side products at every stage remains challenging in multistep solid-phase synthesis.

Biological evaluation of the analogue library did not identify compounds with significantly improved CDK11B inhibition relative to the parent hit. Although hit-to-lead optimization of this scaffold is ongoing outside the present study, the work here shows that the SPS-flow platform can rapidly interrogate chemical space around a hit scaffold through automated multistep synthesis. The programmable CRF-based workflow enabled the preparation of structurally diverse benzodiazepine derivatives within a short time frame and with minimal manual intervention, providing an efficient means to assess synthetic tractability and early SAR during hit evaluation.

Within the explored first-generation design space, the absence of improved potency suggests that the substitutions introduced at the aldehyde-, amino acid-, heteroaryl-, amine-, and diazonium-derived positions did not sufficiently strengthen CDK11B engagement. Even so, the library was able to probe multiple positions on the scaffold under unified digital control, revealing both productive and unproductive diversification vectors and helping to define the current operating window of the SPS-flow sequence. In this context, the study illustrates that negative or neutral SAR can still be generated efficiently and informatively when analogue construction is integrated with programmable multistep synthesis, allowing early scaffold triage and route refinement even when biological outcomes are modest.

3 | Conclusion

We have established an SPS-flow platform that integrates continuous-flow, circulation-flow, and stop-flow operations within an automated workflow, extending earlier predefined-target-specific analogue synthesis to scaffold-level diversification around an HTS-derived benzodiazepine hit. Through programmable CRFs and a sterically tuned triazene linker, the system achieves broad chemical compatibility and reproducibility across a non-peptidic 10–11-step multitransformation sequence under automated control. Applied to a benzodiazepine scaffold identified via HTS, the platform enabled on-demand generation of 42 analogues through 10–11 automated synthesis steps per sequence, each requiring only a single final purification step. The resulting workflow links hit identification, fragment-guided retrosynthetic design, linker and process engineering, CRF-based automation, and analogue generation under unified digital control, defining both the current synthetic operating space of the platform and the limits of the explored SAR.

More broadly, this study demonstrates the potential of SPS-flow as a programmable framework for automated multistep diversification of HTS-derived hit scaffolds. While the present implementation is demonstrated using a benzodiazepine scaffold, the underlying automation architecture may provide a basis for future applications to chemically distinct scaffolds, subject to scaffold-specific retrosynthetic design, reaction optimization, and linker compatibility. Future studies will focus on expanding the accessible chemical space—through alternative linker designs, extended heteroaromatic *N*-substitution patterns, and integration with additional reaction types—to further enhance the utility of SPS-flow in medicinal chemistry workflows.

Author Contributions

Zhenyang Yu: conceptualization, methodology, writing – original draft, writing – review and editing. **Zhi-Qi Zhang:** methodology. **Jiale Wu:** methodology. **Yanbin Zhang:** investigation. **Hwee Ting Ang:** writing – review and editing. **Feng Zhou:** methodology. **Jackie Ang:** data curation. **Mei Yee Wong:** data curation. **Ronald Toh Kuan Hai:** data curation. **Frankie S Mak:** Investigation, Data curation, Supervision, Writing – review and editing, Funding acquisition. **Jie Wu:** conceptualization, funding acquisition, project administration, supervision, writing – original draft, writing – review and editing.

Acknowledgments

We are grateful for the financial support provided by the National Research Foundation, the Prime Minister's Office of Singapore, under its NRF-CRP Programme (Award no. NRF-CRP25-2020RS-0002), and Pfizer (A-8003842-00-00).

Conflicts of Interest

The authors declare no conflicts of interest.

Data Availability Statement

The data that supports the findings of this study are available in the supplementary material of this article.

15213773, 0, Downloaded from https://onlinelibrary.wiley.com/doi/10.1002/anie.15001194 by National University Of Singapore, Wiley Online Library on [29/10/2026]. See the Terms and Conditions (https://onlinelibrary.wiley.com/terms-and-conditions) on Wiley Online Library for rules of use; OA articles are governed by the applicable Creative Commons License

References

1. R. Macarron, M. N. Banks, D. Bojanic, et al., "Impact of High-Throughput Screening in Biomedical Research," *Nature Reviews Drug Discovery* 10 (2011): 188–195, https://doi.org/10.1038/nrd3368.

2. J. P. Hughes, S. Rees, S. Kalindjian, and K. Philpott, "Principles of Early Drug Discovery," *British Journal of Pharmacology* 162 (2011): 1239–1249, https://doi.org/10.1111/j.1476-5381.2010.01127.x.

3. E. Farrant, "Automation of Synthesis in Medicinal Chemistry: Progress and Challenges," *ACS Medicinal Chemistry Letters* 11 (2020): 1506–1513, https://doi.org/10.1021/acsmedchemlett.0c00292.

4. W. R. J. D. Galloway, A. Isidro-Llobet, and D. R. Spring, "Diversity-oriented Synthesis as a Tool for the Discovery of Novel Biologically Active Small Molecules," *Nature Communications* 1 (2010): 80–92, https://doi.org/10.1038/ncomms1081.

5. J.-M. Lu, J.-Z. Pan, Y.-M. Mo, and Q. Fang, "Automated Intelligent Platforms for High-Throughput Chemical Synthesis," *Artificial Intelligence Chemistry* 2 (2024): 100057, https://doi.org/10.1016/j.aichem.2024.100057.

6. B. Burger, P. M. Maffettone, V. V. Gusev, et al., "A Mobile Robotic Chemist," *Nature* 583 (2020): 237–241, https://doi.org/10.1038/s41586-020-2442-2.

7. M. K. Sharma, R. B. Acharya, C. A. Shukla, and A. A. Kulkarni, "Assessing the Possibilities of Designing a Unified Multistep Continuous Flow Synthesis Platform," *Beilstein Journal of Organic Chemistry* 14 (2018): 1917–1936, https://doi.org/10.3762/bjoc.14.166.

8. J. Li, S. G. Ballmer, E. P. Gillis, et al., "Synthesis of Many Different Types of Organic Small Molecules Using One Automated Process," *Science* 347 (2015): 1221–1226, https://doi.org/10.1126/science.aaa5414.

9. A. Adamo, R. L. Beingessner, M. Behnam, et al., "On-Demand Continuous-Flow Production of Pharmaceuticals in a Compact, Reconfigurable System," *Science* 352 (2016): 61–67, https://doi.org/10.1126/science.aaf1133.

10. M. Trobe and M. D. Burke, "The Molecular Industrial Revolution: Automated Synthesis of Small Molecules," *Angewandte Chemie International Edition* 57 (2018): 4192–4214, https://doi.org/10.1002/anie.201710482.

11. S. Steiner, J. Wolf, S. Glatzel, et al., "Organic Synthesis in a Modular Robotic System Driven by a Chemical Programming Language," *Science* 363 (2019): 122–130, https://doi.org/10.1126/science.aav2211.

12. P. Bana, R. Örkényi, K. Lövei, et al., "The Route From Problem to Solution in Multistep Continuous Flow Synthesis of Pharmaceutical Compounds," *Bioorganic & Medicinal Chemistry* 25 (2017): 6180–6189, https://doi.org/10.1016/j.bmc.2016.12.046.

13. S. Chatterjee, M. Guidi, P. H. Seeberger, and K. Gilmore, "Automated Radial Synthesis of Organic Molecules," *Nature* 579 (2020): 379–384, https://doi.org/10.1038/s41586-020-2083-5.

14. R. B. Merrifield, "Solid Phase Peptide Synthesis. I. The Synthesis of a Tetrapeptide," *Journal of the American Chemical Society* 85 (1963): 2149–2154, https://doi.org/10.1021/ja00897a025.

15. R. B. Merrifield, "Automated Synthesis of Peptides," *Science* 150 (1965): 178–185, https://doi.org/10.1126/science.150.3693.178.

16. R. Behrendt, P. White, and J. Offer, "Advances in Fmoc Solid-Phase Peptide Synthesis," *Journal of Peptide Science* 22 (2016): 4–27, https://doi.org/10.1002/psc.2836.

17. R. Porta, M. Benaglia, and A. Puglisi, "Flow Chemistry: Recent Developments in the Synthesis of Pharmaceutical Products," *Organic Process Research & Development* 20 (2016): 2–25, https://doi.org/10.1021/acs.oprd.5b00325.

18. L. Capaldo, Z. Wen, and T. Noël, "A Field Guide to Flow Chemistry for Synthetic Organic Chemists," *Chemical Science* 14 (2023): 4230–4247, https://doi.org/10.1039/D3SC00992K.

19. N. Hartrampf, A. Saebi, M. Poskus, et al., "Synthesis of Proteins by Automated Flow Chemistry," *Science* 368 (2020): 980–987, https://doi.org/10.1126/science.abb2491.

20. C. Li, A. J. Callahan, M. D. Simon, et al., "Fully Automated Fast-flow Synthesis of Antisense Phosphorodiamidate Morpholino Oligomers," *Nature Communications* 12 (2021): 4396–4403, https://doi.org/10.1038/s41467-021-24598-4.

21. F. Wan, C. Hu, P. Xie, et al., "Automated Rapid Synthesis of High-Purity Head-to-Tail Cyclic Peptides via a Diaminonicotinic Acid Scaffold," *Journal of the American Chemical Society* 148 (2026): 986–996, https://doi.org/10.1021/jacs.5c16902.

22. C. Liu, J. Xie, W. Wu, et al., "Automated Synthesis of Prexasertib and Derivatives Enabled by Continuous-Flow Solid-Phase Synthesis," *Nature Chemistry* 13 (2021): 451–457, https://doi.org/10.1038/s41557-021-00662-w.

23. D. Tian, T. W. Tan, R. T. Kuan Hai, et al., "Button-Push on-Demand Synthesis for Rapid Optimization of Antiviral Peptidomimetics," *Journal of the American Chemical Society* 146 (2024): 31321–31329, https://doi.org/10.1021/jacs.4c12834.

24. M. Malumbres, E. Harlow, T. Hunt, et al., "Cyclin-Dependent Kinases: A Family Portrait," *Nature Cell Biology* 11 (2009): 1275–1276, https://doi.org/10.1038/ncb1109-1275.

25. M. Canavese, L. Santo, and N. Raje, "Cyclin Dependent Kinases in Cancer," *Cancer Biology & Therapy* 13 (2012): 451–457, https://doi.org/10.4161/cbt.19589.

26. D. Blazek, "Therapeutic Potential of CDK11 in Cancer," *Clinical and Translational Medicine* 13 (2023): e1201–1204, https://doi.org/10.1002/ctm2.1201.

27. B. T. Kren, G. M. Unger, M. J. Abedin, et al., "Preclinical Evaluation of Cyclin Dependent Kinase 11 and Casein Kinase 2 Survival Kinases as RNA Interference Targets for Triple Negative Breast Cancer Therapy," *Breast Cancer Research* 17 (2015): 19–39, https://doi.org/10.1186/s13058-015-0524-0.

28. J. R. Devlin, B. Martin, N. Bartonicek, et al., "A CDK11-Dependent RNA Polymerase II Pause-Checkpoint Precedes CDK9-Mediated Transition to Transcriptional Elongation," *Molecular Cell* 85 (2025): 3256–3274.e14, https://doi.org/10.1016/j.molcel.2025.08.001.

29. Z. Duan, J. Zhang, E. Choy, et al., "Systematic Kinome shRNA Screening Identifies CDK11 (PITSLRE) Kinase Expression Is Critical for Osteosarcoma Cell Growth and Proliferation," *Clinical Cancer Research* 18 (2012): 4580–4588, https://doi.org/10.1158/1078-0432.CCR-12-1157.

30. Y. Du, D. Yan, Y. Yuan, et al., "CDK11^{p110} Plays a Critical Role in the Tumorigenicity of Esophageal Squamous Cell Carcinoma Cells and Is a Potential Drug Target," *Cell Cycle* 18 (2019): 452–466, https://doi.org/10.1080/15384101.2019.1577665.

31. H. Mohammed, "Advances in Cancer Therapy: A Comprehensive Review of CDK and EGFR Inhibitors," *Cells* 13 (2024): 1656–1692, https://doi.org/10.3390/cells13191656.

32. F. S. Mak, F. M. Ng, P. Anbazhagan, et al., "In Silico-Enabled Discovery and Development of Potent and Selective CDK11 Inhibitors," *ChemMedChem* 21 (2026): e202500882, https://doi.org/10.1002/cmdc.202500882.

33. S. Bräse, D. Enders, J. Köbberling, and F. Avemaria, "A Surprising Solid-Phase Effect: Development of a Recyclable 'Traceless' Linker System for Reactions on Solid Support," *Angewandte Chemie International Edition* 37 (1998): 3413–3415, https://doi.org/10.1002/(SICI)1521-3773(19981231)37:24⟨3413::AID-ANIE3413⟩3.0.CO;2-K.

34. S. L. Dax, *Linker Strategies in Solid-Phase Organic Synthesis* (Wiley VCH, 2009), 1–23, https://doi.org/10.1002/9780470749043.ch1.

35. A. R. Vaino and K. D. Janda, "Solid-Phase Organic Synthesis: A Critical Understanding of the Resin," *Journal of Combinatorial Chemistry* 2 (2000): 579–596, https://doi.org/10.1021/cc000046o.

36. M. Jang, T. Lim, B. Y. Park, and M. S. Han, "Metal-Free, Rapid, and Highly Chemoselective Reduction of Aromatic Nitro Compounds

15213773, 0, Downloaded from https://onlinelibrary.wiley.com/doi/10.1002/anie.15001194 by National University Of Singapore, Wiley Online Library on [29/10/2026]. See the Terms and Conditions (https://onlinelibrary.wiley.com/terms-and-conditions) on Wiley Online Library for rules of use; OA articles are governed by the applicable Creative Commons License

at Room Temperature," *Journal of Organic Chemistry* 87 (2022): 910–919, https://doi.org/10.1021/acs.joc.1c01431.

37. Q. Wang, R. Yin, Z. Wang, Y. Zhang, and J. Wu, "Application of Stop-Flow Micro-Tubing Reactor System in Organic Reaction Development," *Journal of Flow Chemistry* 14 (2024): 97–107, https://doi.org/10.1007/s41981-023-00302-z.

38. H. C. Brown, S. Narasimhan, and Y. M. Choi, "Improved Procedure for Borane-Dimethyl Sulfide Reduction of Tertiary and Secondary Amides in the Presence of Boron Trifluoride Etherate," *Synthesis* 12 (1981): 996–997, https://doi.org/10.1055/s-1981-29677.

39. E. R. Alexander and R. E. Burge Jr., "The Hypophosphorous Acid Deamination of Diazonium Salts in Deuterium Oxide," *Journal of the American Chemical Society* 72 (1950): 3100–3103, https://doi.org/10.1021/ja01163a082.

40. H. H. Hodgson, "The Sandmeyer Reaction," *Chemical Reviews* 40 (1947): 251–277, https://doi.org/10.1021/cr60126a003.

41. A. R. Brown, P. H. H. Hermkens, H. C. J. Ottenheijm, and D. C. Rees, "Solid Phase Synthesis," *Synlett* 1998 (1998): 817–827, https://doi.org/10.1055/s-1998-1813.

Supporting Information

Additional supporting information can be found online in the Supporting Information section.

The authors have cited additional references within the Supporting Information [41].

Supporting File 1: anie75485-sup-0001-Video.mp4.

Supporting File 2: anie75485-sup-0002-SuppMat.pdf.

15213773, 0, Downloaded from https://onlinelibrary.wiley.com/doi/10.1002/anie.1500194 by National University Of Singapore, Wiley Online Library on [29/10/2026]. See the Terms and Conditions (https://onlinelibrary.wiley.com/terms-and-conditions) on Wiley Online Library for rules of use; OA articles are governed by the applicable Creative Commons License